Renormalized semiclassical quantization for rescalable Hamiltonians

Satoshi Takahashi* and Kazuo Takatsuka†
Department of Basic Science, Graduate School of Arts and Sciences, University of Tokyo, Komaba, 153-8902, Tokyo, Japan
(Received 27 May 2004; published 9 November 2004)

A renormalized semiclassical quantization method for rescalable Hamiltonians is proposed. A classical Hamilton system having a potential function that consists of homogeneous polynomials like the Coulombic potential can have a scale invariance in its extended phase space (phase space plus time). Consequently, infinitely many copies of a single trajectory constitute a one-parameter family that is characterized in terms of a scaling factor. This scaling invariance in classical dynamics is lost in quantum mechanics due to the presence of the Planck constant. It is shown that in a system whose classical motions have a self-similarity in the above sense, classical trajectories adopted in the semiclassical scheme interact with infinitely many copies of their own that are reproduced by the relevant scaling procedure, thereby undergoing quantum interference among themselves to produce a quantized spectrum.

DOI: 10.1103/PhysRevA.70.052103 PACS number(s): 03.65.Sq, 05.45.Mt, 31.15.Gy, 11.15.Kc

I. INTRODUCTION

Semiclassical quantization of Coulombic three-body problems, such as the He atom ($p^+e^-e^-$), is an extremely interesting and difficult problem. We have been studying the all-particle dynamics of H_2^+ ($p^+p^+e^-$) and its muon substitution of electrons ($p^+p^+\mu^-$) in terms of a semiclassical theory to examine the validity of the Born-Oppenheimer approximation, a deeper understanding of chemical bonding, and so on. The primary target there is simultaneous quantization of vibronic states. In this problem, two very difficult and interesting problems of classical-quantum correspondence appear explicitly. One is the problem of the energy quantization of chaos, since (not only) the Coulombic three-body system (but also the three-body problem of the gravity field) becomes strongly chaotic very easily. The associated phase space is mostly filled with chaotic zones. The quantization of the energy spectrum for a classically chaotic system has long been one of the central subjects in quantum mechanics and chaos theory, and we still do not have a "perfect" semiclassical methodology that can be applied to many-body systems. The other one is less mathematical but more puzzling. Even if we had a perfect semiclassical method based on classical trajectories, one faces a difficulty that most classical trajectories sampled in the range of to-be-quantized energy are not bounded within the molecular site. Very many trajectories lead to a dissociation of the hydrogen atom (p^+e^-) and p^+. This behavior is more or less characteristic of the Coulomb problem, since a swing-by motion due to a close encounter between the electron and one of the protons can repel the other proton to the asymptotic region. Beside, many quasiseparatrices that distinguish bounded and dissociation motions are densely packed in the narrow zone of the close encounter, and therefore this phenomenon is coupled with chaos. This is not a pathological phenomenon. On the contrary, it has been known for a long time that the escaping of an electron is observed quite frequently in the classical He system. (Even for the three-body gravity problem a similar ejection of a constituent body results quite frequently.) So one is puzzled: How can H_2^+ be quantized to have such a strong chemical bonding with such small number of bounded classical trajectories?

An easy-going answer is to ascribe the quantization to unknown "tunneling trajectories." We do not disagree that nonclassical path could contribute more or less. However, no such huge tunneling effect has been actually quantified before, and no systematic study of which kind of tunneling paths are involved is available in the literature. Moreover, our preliminary study of semiclassical quantization using our semiclassical theory (see below) has successfully produced the ground-state vibronic level without the use of a tunneling path. But at the same time, our spectrum suffers from ghost (spurious) peaks presumably because only a small number of bounded trajectories are available to realize a good interference among quantum phases on the trajectories. For a semiclassical theory to be able to give a correct spectrum, both constructive and destructive quantum interferences are required. In this sense, modern theories of semiclassical quantization such as the Gutzwiller trace formula [1,2] are far more difficult to apply than the old quantization conditions like Bohr's and the EBK conditions [3]. The role of destructive interference has been studied in detail by Inoue-Ushiyama and Takatsuka [4]. It is well known that very many trajectories are necessary to materialize a proper destructive interference in numerical calculations.

This paper is an outcome of the above study of quantization of H_2^+ ($p^+p^+e^-$). While troubled with the aforementioned puzzle, we noticed that the Coulombic potential was scalable in the sense that it is a homogeneous function of the coordinates

$$U(\alpha\vec{r}_1,\ldots,\alpha\vec{r}_N) = \alpha^{-1}U(\vec{r}_1,\ldots,\vec{r}_N), \tag{1}$$

where $\vec{r}_i$ are the relevant coordinates and α is a scaling parameter. For these systems, any single path on this potential has its infinitely many copies in the extended phase space,

*Electronic address: takahasi@mns2.c.u-tokyo.ac.jp
†Electronic address: kaztak@mns2.c.u-tokyo.ac.jp

which are readily reproduced by scaling time, coordinates, momenta, action integrals, and so on. They are essentially indistinguishable from one another in classical mechanics, since they exactly coincide with each other by simply changing the scales. On the other hand, quantum mechanics does not allow such a rescaling, since the Planck constant introduces an absolute measure in phase space. These mutually equivalent trajectories are thereby no longer equivalent in quantum mechanics and make different contributions to quantum interference. What is nice technically is that once a bounded trajectory is found numerically (with the Monte Carlo sampling method, for instance), its infinite copies are generated instantly with use of rescaling.

The present paper is concerned with the methodological aspect of taking an explicit account of the scaling property in semiclassical theories. We show a couple of selected examples of the application, including a system under a one-dimensional Coulomb interaction and of two-dimensional strong chaos. An extensive application to H_2^+ $(p^+p^+e^-)$ along with the physical analyses will be reported elsewhere.

This paper is organized as follows. In Sec. II, we give a simple account of the scale invariance of the classical equations of motion. The invariance is actually installed in semiclassical wave functions and (quasi)correlation functions. We apply this method, called the renormalized semiclassical quantization, to selected examples to show how it works in Sec. III. Section IV concludes this paper with some remarks.

II. CLASSICAL SCALING INCORPORATED INTO SEMICLASSICAL THEORIES

First, we briefly review a scale invariance associated with classical trajectories that arise from a rescalable Hamiltonian [5]. We then incorporate this scaling procedure to a semiclassical wave function and an associated (quasi)correlation function.

A. Scaling property of the classical equations of motion

Let us consider a potential function that is a kth-order homogeneous polynomial in the coordinates satisfying a scaling property such that

$$U(\alpha x_1, \alpha x_2, \ldots, \alpha x_n) = \alpha^k U(x_1, x_2, \ldots, x_n), \tag{2}$$

where α is a constant. The canonical Hamiltonian

$$H(q,p) = \sum_i \frac{p_i^2}{2m_i} + U(x_1, x_2, \ldots, x_n) \tag{3}$$

is considered throughout this paper. A simple scaling transformation in q and t in such a way that $q \to \alpha q, t \to \beta t$ scales all the momenta by a factor α/β and the associated kinetic energy is also changed by a factor α^2/β^2. Since the potential energy is multiplied by α^k, the following relation between α and β,

$$\frac{\alpha^2}{\beta^2} = \alpha^k \quad \text{or} \quad \beta = \alpha^{1-k/2}, \tag{4}$$

leaves the Hamiltonian unchanged except for a factor α^2/β^2.

Thus, a simultaneous scaling

$$(x_1, x_2, \ldots, x_n) \to (\alpha x_1, \alpha x_2, \ldots, \alpha x_n) \tag{5}$$

along with

$$t \to \alpha^{1-k/2} t, \tag{6}$$

with a given α, makes a copy of the original trajectory with a perfectly similar shape in the extended phase space (q,p,t) with accordingly transformed momentum, total energy, and the action integral as follows:

$$p_i \to \alpha^{k/2} p_i, \quad E \to \alpha^k E, \quad S \to \alpha^{1+k/2} S. \tag{7}$$

A continuous change of the scaling parameter generates infinitely many copies of the "original," which form a one-parameter family. This is because the extended phase space does not have a characteristic size as in fractal geometry. Hence, any size of the geometry can be equally acceptable as a physical quantity. A very useful fact for our later purposes is that once one of these trajectories is numerically obtained, all the other family members are generated automatically using a simple set of arithmetic operations.

Incidentally, for a map M_α satisfying

$$M_\alpha : \{q,p,t,E,S\} \to \{\alpha q, \alpha^{k/2} p, \alpha^{1-k/2} t, \alpha^k E, \alpha^{1+k/2} S\}, \tag{8}$$

it is obvious that a set of $M=\{M_\alpha\}$ makes an Abelian group M such that (i) $M_\alpha M_\beta = M_\beta M_\alpha = M_{\alpha\beta} \in M$, (ii) $M_\alpha(M_\beta M_\gamma) = (M_\alpha M_\beta) M_\gamma$, (iii) $I = M_1$ (the identity element), and (iv) $M_\alpha^{-1} = M_{\alpha^{-1}}$.

B. Scaling property incorporated into semiclassical theory

1. Introduction of the scale invariance to the semiclassical kernel

We now introduce the above scale invariance of classical mechanics into the semiclassical kernel and the relevant correlation function. First let us consider the semiclassical Feynman kernel in the initial value representation [6–8] (see Refs. [9–12] for the relevant progress)

$$K_{\rm sc}(q,q_0,t) = (2\pi i\hbar)^{-N/2} \int \delta(q - q_t) \left| \frac{\partial q_t}{\partial p_0} \right|^{1/2} \times \exp\left(\frac{i}{\hbar} S(q_t,q_0,t) - i\pi \frac{\lambda_t}{2} \right) dp_0, \tag{9}$$

where S is the classical action function and λ_t is the Maslov index in this representation. The semiclassical wave function at a desired time is obtained with the kernel

$$\Psi_{\rm sc}(q,t) = \int dq_0 K_{\rm sc}(q,q_0,t) \Psi(q_0,0), \tag{10}$$

and the associated semiclassical correlation function is written as

$$\langle\Psi(0)|\Psi(t)\rangle = (2\pi i\hbar)^{-N/2}\int \Psi^*(q_t)\Psi(q_0)\left|\frac{\partial q_t}{\partial p_0}\right|^{1/2} \times \exp\left(\frac{i}{\hbar}S(q_t,q_0,t) - i\pi\frac{\lambda_t}{2}\right)dq_0dp_0. \quad (11)$$

The Fourier transform of it gives an energy spectrum associated with this wave function—that is,

$$P(E) = \int dt\langle\Psi(0)|\Psi(t)\rangle\exp\left[\frac{i}{\hbar}Et\right]. \quad (12)$$

Let us consider a rescalable system with a potential function of the degree of homogeneity k. The similarity transformation of a geometry in the extended phase space is induced as in Eqs. (5), (6), and (7). If trajectories in the kernel, Eq. (9), are transformed as above, the kernel is accordingly transformed to

$$K_{\rm sc}(\alpha q,\alpha q_0,\alpha^{1-k/2}t) = (2\pi i\hbar)^{-N/2}\int \delta(\alpha q - \alpha q_{\alpha^{1-k/2}t}) \times \left|\frac{\partial(\alpha q_{\alpha^{1-k/2}t})}{\partial(\alpha^{k/2}p_0)}\right|^{1/2} \times \exp\left(\frac{i}{\hbar}S(\alpha q_{\alpha^{1-k/2}t},\alpha q_0,\alpha^{1-k/2}t) - i\pi\frac{\lambda_{\alpha^{1-k/2}t}}{2}\right)d(\alpha^{k/2}p_0). \quad (13)$$

Here in this expression, an exact copy of a reference trajectory in the extended phase space is made use of—that is,

$$(q,p,t) \to (\alpha q,\alpha^{k/2}p,\alpha^{1-k/2}t). \quad (14)$$

Any copied trajectory has an exact one-to-one correspondence with the original one. However, in order to evaluate the correlation function as in Eq. (12), the time should not be scaled as $\alpha^{1-k/2}t$ but is to be kept to t. Define a time $s(t,\alpha)$ so as to satisfy

$$\alpha^{1-k/2}s(t,\alpha) = t. \quad (15)$$

The reference trajectory is required to run as long as $s(t,\alpha)$ to generate a scaled path of the time length of t. The kernel we need in place of Eq. (13) is now

$$K_{\rm sc}(\alpha q,\alpha q_0,t) = (2\pi i\hbar)^{-N/2}\int \delta(\alpha q - \alpha q_{\alpha^{1-k/2}s(t,\alpha)}) \times \left|\frac{\partial(\alpha q_{\alpha^{1-k/2}s(t,\alpha)})}{\partial(\alpha^{k/2}p_0)}\right|^{1/2} \times \exp\left(\frac{i}{\hbar}S(\alpha q_{\alpha^{1-k/2}s(t,\alpha)},\alpha q_0,\alpha^{1-k/2}s(t,\alpha)) - i\pi\frac{\lambda_{\alpha^{1-k/2}s(t,\alpha)}}{2}\right)d(\alpha^{k/2}p_0). \quad (16)$$

We intentionally leave the suffix $\alpha^{1-k/2}s(t,\alpha)$ instead of t to remind the reader that the reference trajectory should be run as long as the time length $s(t,\alpha)$ to produce the copied trajectory

$$(q,p,s(t,\alpha)) \to (\alpha q,\alpha^{k/2}p,t). \quad (17)$$

Under this understanding, we simply write $\alpha^{1-k/2}s(t,\alpha)$ as t in what follows such that

$$K_{\rm sc}(\alpha q,\alpha q_0,t) = (2\pi i\hbar)^{-N/2}\int \delta(\alpha q - \alpha q_t)\left|\frac{\partial(\alpha q_t)}{\partial(\alpha^{k/2}p_0)}\right|^{1/2} \times \exp\left(\frac{i}{\hbar}S(\alpha q_t,\alpha q_0,t) - i\pi\frac{\lambda_t}{2}\right)d(\alpha^{k/2}p_0). \quad (18)$$

It is obvious that even if the classical quantities are all scale invariant, the phase term (the exponential function) is not, since the Planck constant is not rescaled. Therefore the kernel itself is not scale invariant. Let us rewrite the kernel in Eq. (18) symbolically as

$$K^\alpha_{\rm sc}(q,q_0,t) = K_{\rm sc}(\alpha q,\alpha q_0,t), \quad (19)$$

which is a kernel representing the scale α. Using this kernel we define the following wave packet state $\Psi^\alpha_{\rm sc}(q,t)$:

$$\Psi^\alpha_{\rm sc}(q,t) = \int d(\alpha q_0)K^\alpha_{\rm sc}(q,q_0,t)\Psi(\alpha q_0,0), \quad (20)$$

which also represent a wave packet at the scale of α. To build a wave packet that is scale invariant one may integrate $\Psi^\alpha_{\rm sc}(q,t)$ over the scaling parameter α to pick the entire information from all the (mathematically) possible scales such that

$$\Phi_{\rm sc}(q,t) \equiv \int_0^\infty d\alpha\Psi^\alpha_{\rm sc}(q,t) = \int_0^\infty d\alpha\int d(\alpha q_0)K^\alpha_{\rm sc}(q,q_0,t) \times\Psi(\alpha q_0,0). \quad (21)$$

It is easy to show that this new wave function is also scale invariant up to a constant, since

$$\Phi_{\rm sc}(\gamma q,t) = \frac{1}{\gamma}\int_0^\infty d(\gamma\alpha)\Psi^{\gamma\alpha}_{\rm sc}(q,t) = \frac{1}{\gamma}\Phi_{\rm sc}(q,t). \quad (22)$$

A time correlation function of a wave packet $\Psi^\alpha_{\rm sc}(q,t)$ at the scale of α is

$$\langle\Psi^\alpha_{\rm sc}(0)|\Psi^\alpha_{\rm sc}(t)\rangle. \quad (23)$$

If the complete set of classical trajectories could be sampled in practice, the resultant spectrum should not depend on the scaling parameter. However, the reality is far from this ideal situation. On the contrary, it is quite often not easy to pick good trajectories as we stated in the Introduction. Thus, making use of a set of reference trajectories, one can extend the range of sampling space by scanning the scaling parameter such that

$$\int_0^\infty d\alpha \langle \Psi_{\rm sc}^\alpha(0)|\Psi_{\rm sc}^\alpha(t)\rangle. \tag{24}$$

This is a semiclassical correlation function to be Fourier transformed. The merit of this procedure is obvious: The effect of infinitely many associated classical paths can be readily taken into account once a classical trajectory is found numerically. The more difficult is a classical dynamics under study, the more significant becomes this theoretical advantage.

In practice, however, one cannot carry out the integral over the scaling parameter α in the range of $[0,\infty]$. Rather it is a usual practice to make a wave packet within a finite range $[\alpha_1,\alpha_2]$ such that

$$\Phi_{\rm sc}^{[\alpha_1,\alpha_2]}(q,t) = \int_{\alpha_1}^{\alpha_2} d\alpha \Psi_{\rm sc}^\alpha(q,t). \tag{25}$$

By choosing an appropriate range $[\alpha_1,\alpha_2]$, one can produce a wave packet in a corresponding range of the classical energy to make an efficient calculation of the eigenvalues of interest. Similarly the correlation function is also taken in a finite range:

$$\int_{\alpha_1}^{\alpha_2} d\alpha \langle \Psi_{\rm sc}^\alpha(0)|\Psi_{\rm sc}^\alpha(t)\rangle. \tag{26}$$

Formally the above procedure is good enough for practical applications as far as the introduction of the scaling invariance is concerned. However, we do not actually resort to the standard semiclassical Feynman kernel in the following part of this paper, since quite often it fails to give a good resolution of spectrum in the domain of classical chaos. The reason for this difficulty is now well known that the amplitude factor $|\partial q_t/\partial p_0|^{1/2}$ appearing in Eq. (11) becomes exponentially large as time proceeds in a form

$$|\partial q_t/\partial p_0|^{1/2} \sim \exp\left(\frac{K}{2}t\right), \tag{27}$$

where K is the so-called local Liapunov entropy [13]. A Fourier transform of the concomitant exponential increase of the correlation function results in a very bad resolution of a spectrum due to the Lorentzian widths depending on the magnitude of K. Recently a class of semiclassical quasicorrelation functions has been proposed for the energy quantization of chaos, with which the exponentially diverging amplitude factor is not associated [14,15]. It is confirmed that this quasicorrelation function, called the amplitude-free quasicorrelation function type II (AFC-II) [15,24], is extremely powerful in the practical quantization of chaotic systems. It can be readily applied to multidimensional systems having a generic potential of more than two dimensions. In what follows therefore, we use the AFC-II to examine the validity and effects of the scale invariance.

2. Introduction of the scale invariance to the action decomposed function

We begin with the following action decomposed function (ADF) specified by the initial momentum p_0 of classical trajectories [17]:

$$\Psi_{p_0}(q,t) = \int dq_0 \delta(q - q_t(q_0,p_0)) F(q_0,0) \left|\frac{\partial q_t}{\partial q_0}\right|^{1/2} \times \exp\left[\frac{i}{\hbar}S_2(q_t,p_0,t) - \frac{i\pi M}{2}\right], \tag{28}$$

where the derivative $\partial q_t/\partial q_0$ is taken under the fixed initial momentum p_0, S_2 is the classical action function that satisfies the Hamilton-Jacobi equation as the F_2 type generating function of Goldstein [16], and M is the Maslov index in this representation which counts the number of zeros of the Jacobian determinant $\partial q_t/\partial q_0$ up to the degeneracy. The way of constructing ADF and its general properties, merits, limitation, and so on should be referred to Refs. [4,17].

If paths constituting the ADF are rescaled by a parameter α and other variables are changed as in Eqs. (6) and (7), the accordingly transformed ADF is written as

$$\begin{aligned}
\Psi_{p_0}^\alpha(q,t) &= \Psi_{a^{k/2}p_0}(\alpha q, \alpha^{1-k/2}s(t,\alpha)) \\
&= \int d(\alpha q_0)\delta(\alpha q - q_{\alpha^{1-k/2}s(t,\alpha)}(\alpha q_0, \alpha^{k/2}p_0)) \\
&\quad \times F(\alpha q_0,0)\left|\frac{\partial(\alpha q_{\alpha^{1-k/2}s(t,\alpha)})}{\partial(\alpha q_0)}\right|^{1/2} \\
&\quad \times \exp\left[\frac{i}{\hbar}S_2(\alpha q_{\alpha^{1-k/2}s(t,\alpha)}, \alpha^{k/2}p_0, \alpha^{1-k/2}s(t,\alpha)) \right. \\
&\quad \left. - \frac{i\pi M(\alpha q_0, \alpha q_{\alpha^{1-k/2}s(t,\alpha)})}{2}\right] \\
&= \int d(\alpha q_0)\delta(\alpha q - q_t(\alpha q_0, \alpha^{k/2}p_0)) \\
&\quad \times F(\alpha q_0,0)\left|\frac{\partial(\alpha q_t)}{\partial(\alpha q_0)}\right|^{1/2} \\
&\quad \times \exp\left[\frac{i}{\hbar}S_2(\alpha q_t, \alpha^{k/2}p_0, t) - \frac{i\pi M(\alpha q_0, \alpha q_t)}{2}\right].
\end{aligned} \tag{29}$$

We integrate this semiclassical wave function over the scaling parameter α:

$$\Phi_{p_0}(q,t) \equiv \int d\alpha \Psi_{p_0}^\alpha(q,t). \tag{30}$$

Again this wave function is scale invariant, since it is a simple "sum" over the entire range of the scaling parameter. We call it the renormalized ADF.

The scale-invariant amplitude-free quasicorrelation function based on the $\Psi_{p_0}^\alpha(q,t)$ is

$$C_{p_0}(-t,t) = \int d\alpha \langle \Psi^{\alpha}_{p_0}(-t) | \Psi^{\alpha}_{p_0}(t) \rangle$$
$$= \int d\alpha \int\int dq_{01} dq_{02} \delta(\alpha q_{-t} - \alpha q_t) F^*(\alpha q_{01}, 0)$$
$$\times F(\alpha q_{02}, 0) \left| \frac{\partial q_{-t}}{\partial q_{01}} \right|^{1/2*} \left| \frac{\partial q_t}{\partial q_{02}} \right|^{1/2}$$
$$\times \exp\left[-\frac{i}{\hbar} S_2(\alpha q_{-t}, \alpha^{k/2} p_0, -t) \right.$$
$$\left. + \frac{i\pi M(\alpha q_{01}, \alpha q_{-t})}{2} \right] \exp\left[\frac{i}{\hbar} S_2(\alpha q_t, \alpha^{k/2} p_0, t) \right.$$
$$\left. - \frac{i\pi M(\alpha q_{02}, \alpha q_t)}{2} \right], \tag{31}$$

in which the interference at all possible scales is taken into account. (Note that the correlation is taken between t and $-t$, but not 0 and t.)

To improve this quasicorrelation, we further proposed another amplitude-free quasicorrelation function II as [15]

$$C_{II}(t) = \int dq_0 |F(q_t, 0) F(q_0, 0)|$$
$$\times \exp\left[\frac{i}{\hbar} S_1(q_t, q_0, t) - i\frac{\pi}{2} M(q_0, q_t) \right]. \tag{32}$$

The momentum p_0 at $t=0$ should be selected to be zero, which picks only the so-called turn-back orbits as sampling paths [15]. The functional form of a wave packet to be propagated is usually chosen as a Gaussian function

$$F_{\lambda}(q,0) = \exp[-\lambda(q - q_c)^2]. \tag{33}$$

This rather sharp Gaussian function imposes the condition of weak periodicity on the turn-back orbits [15]. Our desired correlation function that takes account of the scaling property is

$$C_{\mathrm{re}}(t) = \int d\alpha \int d(\alpha q_0) |F_{\lambda/\alpha^2}(\alpha q_t, 0) F_{\lambda/\alpha^2}(\alpha q_0, 0)|$$
$$\times \exp\left[\frac{i}{\hbar} S_1(\alpha q_t, \alpha q_0, t) - i\frac{\pi}{2} M(\alpha q_0, \alpha q_t) \right], \tag{34}$$

which we call the renormalized AFC in the following. Notice that we scale the exponent of the initial Gaussian such that

$$F_{\lambda/\alpha^2}(\alpha q_0, 0) = \exp\left[-\frac{\lambda}{\alpha^2} (\alpha q_0 - \alpha q_c)^2 \right] = \exp\left[-\lambda (q_0 - q_c)^2 \right]. \tag{35}$$

This is a requirement that the Gaussian function should have the same size in the space of the reference trajectories, if the scaled trajectories $\{\alpha q\}$ are scaled back to the original space as $\{\alpha^{-1} \alpha q\}$. In the quasicorrelation function, Eq. (34), we can thus impose a coherent quantum interference between the phases arising from infinitely many copied trajectories. As in the original AFC-II, the quasicorrelation function of Eq. (34) is not associated with the amplitude factor in contrast to the kernel that has $|\partial q_t / \partial p_0|^{1/2}$ in Eq. (11), which grows exponentially as time proceeds and thereby hampering the resolution of the spectrum. Therefore it is possible to apply $C_{\mathrm{re}}(t)$ not only to regular systems but to highly chaotic ones. Comparison between the AFC's and the kernel-based correlation function has been made in a detail in [15]. Now, we are ready to apply the renormalized AFC to one- and two-dimensional rescalable systems and show how effectively it works. Although, at a first glance, the integration over the α coordinate in Eq. (34) is redundant, this is not the case. We will explain this aspect below in a detail with the help of numerical results.

III. PRACTICAL APPLICATION TO RESCALABLE HAMILTONIANS

This section is devoted to applications of the renormalized AFC to a couple of selected systems whose Hamiltonians are scalable. In all cases we set the mass of particles to unity without loss of generality. In both one- and two-dimensional cases, we chose $F(q,0)$ to be the Gaussian wave packet described above. We performed the practical calculations of the energy spectra with the following procedure: (i) Calculate one reference trajectory (one set of trajectories) starting from a certain initial condition(s) and store the time evolution data of the coordinate, the action integral, and the Maslov index. (ii) Generate copies of the reference trajectory by the scaling procedure described above. (iii) Compute the renormalized AFC with Eq. (34) in terms of these copies along with the reference one and evaluate its associated spectrum by Fourier transformation over the time. The above procedure is essentially the same as preparing a number of initial wave packet having geometrically the same shape in the configuration space at a time. In this way, it is possible to calculate the semiclassical wave packets in a variety of sizes. To keep the renormalized ADF [Eq. (30)] exactly scale invariant, the integration over the scaling parameter α has to be taken theoretically from 0 to $+\infty$. However, since it is impossible to carry out the integral of α in the range of $[0,\infty]$ in numerical calculations, we approximate it in terms of a quadrature over a limited range of α (see below). As shown below, the choice of the range of the scaling parameter is practically important to take a good account of quantum interference among self-similar trajectories.

In the calculation of the time evolution of classical trajectories and the stability matrix, we used the locally analytic integrator [18], which is accurate and fast to solve the ordinary differential equations.

A. x^4-type potential

First we consider the following Hamiltonian with a quartic potential:

$$H = \frac{1}{2} p^2 + \frac{1}{4} x^4. \tag{36}$$

This simple system is scalable and yet anharmonic, which is nice to begin with. If the coordinate and time are transformed

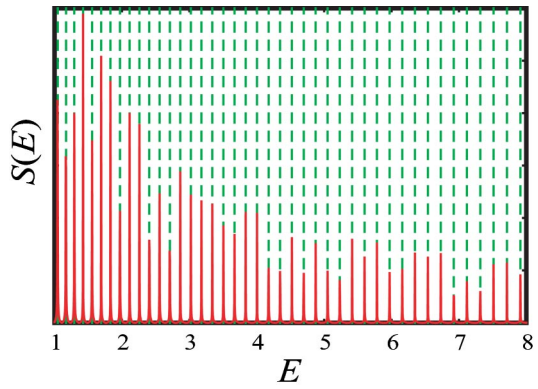

FIG. 1. (Color online) (Green and dotted lines) Energy levels obtained with the wave packet dynamics for the potential $x^4/4$. (Red) Energy levels obtained with the renormalized AFC, which is based on only one reference classical trajectory of the initial condition $(x_0,p_0)=(1.0,0)$.

as $x\to\alpha x$ and $t\to\alpha^{-1}t$, the equation of motion is left unchanged and the Hamiltonian is transformed as

$$H' = \frac{1}{2}\left(\frac{d(\alpha x)}{d(\alpha^{-1}t)}\right)^2 + \frac{1}{4}(\alpha x)^4 = \alpha^4\left[\frac{1}{2}\left(\frac{dx}{dt}\right)^2 + \frac{1}{4}x^4\right] = \alpha^4 H. \tag{37}$$

The momentum, the energy, and the action integral are transformed as $p\to\alpha^2 p, E\to\alpha^4 E$, and $S\to\alpha^3 S$. Here we set the Planck constant $\hbar=0.1$. The renormalized AFC has been calculated using only one reference (yet arbitrary) classical trajectory whose initial condition is $(x_0,p_0)=(1.0,0)$ and $E=0.25$. We set the scaling parameter α to be in a range [1.0, 3.0], which is divided into 2000 tiny subintervals to sample the scaled 2000 paths and to carry out the quadrature over α. The energy range of those scaled trajectories is from $E=0.25$ to $E=20.25$.

In Fig. 1 we show the thus obtained semiclassical power spectrum (red one) along with the full quantum spectrum based on a wave packet propagation (green dotted lines). Table I lists the estimated eigenvalues with the present method for selected states along with those given by the quantum wave packet method and the EBK condition. Since the renormalized AFC and quantum wave packet propagation make use of the fast Fourier transform (FFT), the energy resolution is limited to 0.000 48 in our choice of time length.

TABLE I. Eigenvalues of the one-dimensional quartic potential $x^4/4$.

n[a]	Quantum wave packet[b]	EBK	Renormalized AFC[b]
10	0.9257	0.9254	0.9254
20	2.2584	2.2582	2.2581
30	3.8357	3.8355	3.8356
40	5.5981	5.5980	5.5979
50	7.5131	7.5130	7.5129

[a]The quantum number.
[b]Resolution limit for the energy in this FFT is 0.00048.

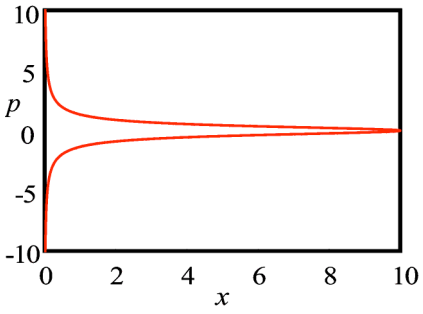

FIG. 2. (Color online) A classical trajectory in phase space for the potential $-1/|x|$. The energy is $E=-0.1$. The appearance of infinity at $x=0$ makes a characterisitic geometry of the paths.

(More accurate values beyond this limit can be obtained in terms of a simple method [19], which actually has been used in this table.) Although the resultant accuracy depends on the number of sampling points in a given parameter space $[\alpha_1,\alpha_2]$, the agreement observed in Fig. 1 is almost perfect in this resolution. Since the present method does not run many trajectories, the associated calculations are by far easier and less time consuming. Note that we can obtain in principle all the energy levels from only one classical trajectory by extending the range of α.

B. One-dimensional Coulomb potential

Next we consider a "one-dimensional hydrogen atom." It consists of an electron moving in the one-dimensional Coulomb potential $-e^2/|x|$, where e is the electric charge and $|x|$ is the distance from the proton. The quantum energy levels of the one-dimensional hydrogen atom have been calculated analytically by Loudon [20]. It is shown that the one-dimensional and three-dimensional hydrogen atoms have common energy levels, which are

$$E_n = -\frac{m_e e^2}{2\hbar}\frac{1}{n^2}, \tag{38}$$

where m_e denotes the mass of the electron (we do not use the reduced mass for a comparison below) and n is a positive integer.

We considered the one-dimensional Coulomb system

$$H = \frac{1}{2}p^2 - \frac{1}{|x|}. \tag{39}$$

Here we use atomic units ($\hbar=m_e=e=1$). In the quantum mechanical treatment, Loudon set a small cutoff and rounded off the Coulomb potential to remove the singularity at the origin [20]. In our semiclassical treatment, this problem is treated in the following picture. The electron with unit mass comes periodically close to the infinitely massive proton due to the Coulomb attraction. When the electron reaches the origin with an infinitely large momentum (the electron reaches the origin in a finite time), an elastic collision occurs there and the electron goes back along the path on which it has come. An example of a classical trajectory in phase space is drawn in Fig. 2. Quantizing the area of a phase space

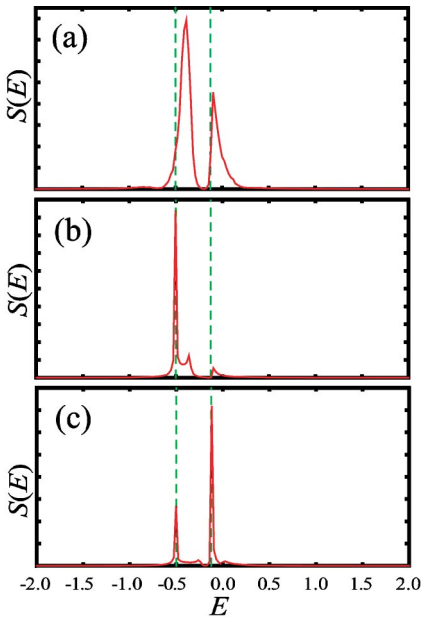

FIG. 3. (Color online) (a) Energy spectra for the potential $-1/|x|$ obtained in terms of the normal AFC-II [Eq. (32)] with 5000 trajectories. Panels (b) and (c) show the spectra due to the renormalized AFC [Eq. (34)] (red lines), which are calculated with a single reference trajectory and its copies. For (b) the range of the scaling parameter is from 0.1 to 0.5 and the number of copies is 4000, while for (c) the range is from 0.01 to 0.81 and 8000 copies have been used. The time length for the FFT is 262.144 for all these cases. The resultant energies given in panel (c) are −0.498 (exact value is −0.500) for $n=1$ and −0.125 (exact value is −0.125) for $n=2$. The green and dotted lines are the analytical solutions of quantum mechanical energy for the one-dimensional hydrogen atom.

region surrounded by the p axis and the trajectory by means of the EBK quantization condition, we confirmed the validity of the semiclassical quantization.

If the coordinate and time are transformed as $x \to \alpha x$ and $t \to \alpha^{3/2} t$, the Hamiltonian becomes

$$H' = \frac{1}{2}\left(\frac{d(\alpha x)}{d(\alpha^{3/2}t)}\right)^2 - \frac{1}{|\alpha x|} = \alpha^{-1}\left[\frac{1}{2}\left(\frac{dx}{dt}\right)^2 - \frac{1}{|x|}\right] = \alpha^{-1}H \tag{40}$$

and other mechanical quantities are transformed as $p \to \alpha^{-1/2}p$, $E \to \alpha^{-1}E$, and $S \to \alpha^{1/2}S$. In Fig. 3 we show three energy spectra obtained with the normal AFC-II, Eq. (32), panel (a), and the renormalized AFC, Eq. (34), panels (b) and (c). To carry out the calculation of the normal AFC-II, Fig. 3(a), we chose $F_\lambda(q_0,0)$ as a Gaussian as described above with minimum uncertainty—i.e., $\lambda = 1/(2\hbar)$—the center of which was placed at $q_c=4.0$ (the corresponding classical energy with $p_0=0$ is $E_{\rm cl}=-0.25$). The number of the trajectories actually run is 5000. As is seen, the resultant spectrum is not good. The Coulomb system is thus difficult even in a one-dimensional system. One major reason for this bad result is that the position of the initial wave packet ($q_c=4.0$) was actually not good, since this classical energy $E_{\rm cl}=-0.25$ is not close to a quantum eigenvalue. (We intentionally chose this condition to illustrate the intrinsic difficulty.) However, a more serious defect of this result is that one of the peaks has a large tail in the positive-energy region, where no bound state can be made. This is a ghost component due to an insufficient destructive interference among the trajectories [4]. As we have already stressed above, both constructive and destructive interferences have to be well realized in semiclassical calculations. To delete this peak, however, a tremendous number of trajectories should be necessary.

We next show the power spectra, Figs. 3(b) and 3(c), which have been obtained in terms of the renormalized AFC of Eq. (34). In doing so, we first generated a single reference trajectory that has an initial condition $(x_0,p_0)=(10.0,0)$. For the spectrum of Fig. 3(b), we set the integration range of α as $[\alpha_1,\alpha_2]=[0.1,0.5]$, which is divided into 4000 pieces to generate the copies of the reference path. In this way, 4000 trajectories have been produced operationally in the physical ranges from $x_0=1.0$ to $x_0=5.0$ and from $E=-1.0$ to $E=-0.2$. The exact quantum mechanics gives two eigenvalues at $E=-0.5$ and $E=-0.125$ as indicated with the (green) dotted lines in Fig. 3.

As observed very clearly in Fig. 3(b), the spectrum has been drastically improved with this simple method. In particular, the peak at $E=-0.5$ has been completely reproduced. Also, the computational time has been dramatically reduced, although this single dimensional case is obviously not a good system to demonstrate computational efficiency. Nevertheless, this spectrum is still contaminated by a small spurious peak, which suggests again that the Coulombic system is really tough against semiclassical quantization.

For a more efficient inclusion of the destructive interference, we have widened the integration range of the scaling parameter α to $[\alpha_1,\alpha_2]=[0.01,0.81]$ and divided into 8000 pieces, which corresponds to the physical interval from $x_0=0.1$ ($E=-10.0$) to $x_0=8.1$ ($E=-0.12$). As is seen in the panel (c), the resultant spectrum is far better and almost perfect.

The above comparative study shows that the integration over α in $C_{\rm re}(t)$, Eq. (34), is not redundant with respect to the integration in q_0 but it has an effect to improve the quality of the correlation function itself: By integration over α in Eq. (34), the central position of the Gaussian, q_c of Eq. (33), is also varied. For a fixed AFC-II, the trajectories are sampled so that they actually mimic the Gaussian function $\exp[-\lambda(q-q_c)^2]$. Therefore, a bad choice of q_c leads to an inefficient sampling of trajectories and damages the resultant spectrum. On the other hand, by taking account of the scaling explicitly, the sampled trajectories (actually produced by the copying procedure) in the scaled scheme, which also shifts the position of the initial Gaussian function as in the wavelet transformation, can cover the wider space and materialize the better constructive and destructive interferences.

C. x^2y^2-type potential (quartic potential)

For a two-dimensional case, we study the Hamiltonian

$$H = \frac{1}{2}p_x^2 + \frac{1}{2}p_y^2 + \frac{1}{2}x^2y^2 + \frac{\beta}{4}x^4 + \frac{\beta}{4}y^4, \tag{41}$$

with $\beta=0.01$. This system is known to be strongly chaotic and has been studied by many authors. Eckhardt, Hose, and

Pollak examined quantum energies and time-dependent wave functions [21]. They made semiclassical estimates of the energies of certain states based on an adiabatic separation between the motions along the least unstable periodic orbits and those perpendicular to them. Kay applied the semiclassical initial-value representation of a wave function in terms of the Herman-Kluk propagator [22]. In his procedure, chaotic trajectories whose accuracy is deteriorated in the semiclassical calculation were removed. Campolieti and Brumer showed that the energy spectrum of this quartic oscillator can be calculated by the method of stationary-phase Monte Carlo (SPMC) integration [23]. These semiclassical calculations basically showed good agreement with the quantum values, but a large number of trajectories are required to reduce the noise. For instance, these authors [22,23] reported that about $\sim 5\times 10^5$ trajectories were used in their calculations.

The primary aim of the present paper is to show how the renormalized AFC, Eq. (34), works for this rescalable system, and therefore no comparison with the above semiclassical methods are to be made. The scaling property of the system is as follows. If the coordinate and the time are transformed as $x\rightarrow \alpha x$ and $t\rightarrow \alpha^{-1}t$, the Hamiltonian becomes

$$\begin{aligned} H' &= \frac{1}{2}\left(\frac{d(\alpha x)}{d(\alpha^{-1}t)}\right)^2 + \frac{1}{2}\left(\frac{d(\alpha y)}{d(\alpha^{-1}t)}\right)^2 + \frac{1}{2}(\alpha x)^2(\alpha y)^2 + \frac{\beta}{4}(\alpha x)^4 \\ &\quad + \frac{\beta}{4}(\alpha x)^4 \\ &= \alpha^4\left[\frac{1}{2}\left(\frac{dx}{dt}\right)^2 + \frac{1}{2}\left(\frac{dy}{dt}\right)^2 + \frac{1}{2}x^2y^2 + \frac{\beta}{4}x^4 + \frac{\beta}{4}y^4\right] \\ &= \alpha^4 H \end{aligned} \tag{42}$$

and other mechanical quantities are transformed as $p\rightarrow \alpha^2 p$, $E\rightarrow \alpha^4 E$, and $S\rightarrow \alpha^3 S$. Here we set the Planck constant $\hbar=0.1$. In the calculation of the Maslov index along classical trajectories, the propagation of the stability matrix suffers from serious numerical instability due to the strong chaos. We therefore used the geometrical evaluation method of the Maslov index, which was devised by the present authors [24]. This method has been shown to be very practical even for multidimensional and/or chaotic systems. We compare the semiclassical spectrum with that obtained by means of the quantum wave packet dynamics to show that (i) one does not have to increase the number of classical trajectories to remove the noise in the spectrum, and (ii) using Eq. (34), energy levels covering a broader range are obtained with a single set of trajectories.

The Gaussian function of Eq. (33) to carry out our semiclassical calculations is centered at $(x_0,y_0)=(2.939,0.272)$ $(E=0.505)$, and $\lambda=1/(2\hbar)$. We first perform the normal AFC-II calculations without use of the scaling property. Here 500 classical trajectories are generated in terms of the importance sampling to mimic this Gaussian function. The initial momentum of all these trajectories is set to zero, $p_0=0$. The resultant spectrum is shown in Fig. 4(a) (red curve) along with the spectrum based on the full quantum wave packet dynamics (green and dotted curve). Since there are different dynamical origins that give birth to the spectral lines in this system, a single wave packet dynamics does not reproduce the entire spectral lines in a given energy range. We therefore calculated the correlation functions with use of several wave packets and obtained their spectral series. The green curves in Fig. 4 are superposition of these (power) spectra. Besides, the height of the semiclassical spectral lines should not be compared with the quantum values anyway, since the AFC has already lost information relevant to the absolute value of the correlation function [14,15]. An inspection shows that although some of the semiclassical energies are in good agreement with the quantum values, the overall agreement is rather poor. In particular, the high-energy components are actually bad. This is not surprising in view of such a small number of trajectories used.

Here we make use of the scaling property and the renormalized AFC of Eq. (34). For each of 500 trajectories generated above, we have made 10 000 copies so that the energy of the center of the wave packet (q_c) ranges from $E=0.3$ to $E=1.3$. Thus 5 000 000 paths in total have been taken into account without much additional labor. As confirmed in the panel (b), the semiclassical spectrum (the red curve) has been dramatically improved. It is remarkable that the high-energy components show such a better performance without practically generating the actual classical trajectories. The accuracy of the spectrum should depend on the quality and topology of the initially sampled reference trajectories and the range of the scaling parameter α to be taken. Also the AFC-II we have used in this paper has a range of validity as a semiclassical theory. However, the validity and advantage of application of the scaling property in any semiclassical theory should be distinguished from these specific practices.

IV. CONCLUSION

In this paper, we have investigated the semiclassical energy spectra for systems having classical scale invariance. We have shown a practical procedure to introduce the scale invariance into the semiclassical wave function and the (quasi)correlation function. Through this procedure the effect of quantum interference among the rescaled copies of a single trajectory is naturally taken into account. Consequently, only a small set of reference trajectories actually can bring about a huge (theoretically infinite) number of quantum interferences. The numerical examples have demonstrated these facts and suggest how to use the scaling procedure in practice. We have studied only the energy quantization in this paper. However, a similar idea can be readily adopted for more general semiclassical purposes such as the calculations of wave functions.

Although the present paper is somewhat involved in a technical aspect of semiclassical theory, neither the accuracy nor sampling technique in Monte Carlo integrations has been our main concern. Rather, our interest in the scale-invariant semiclassical theory originated from the study of the (highly chaotic) classical motion in Coulomb three-body systems such as H_2^+ $(p^+p^+e^-)$. Not only are these systems strongly chaotic but also it is generally difficult to find a sufficient number of classical trajectories that are bound to represent the molecule state. It is virtually impossible for an actual

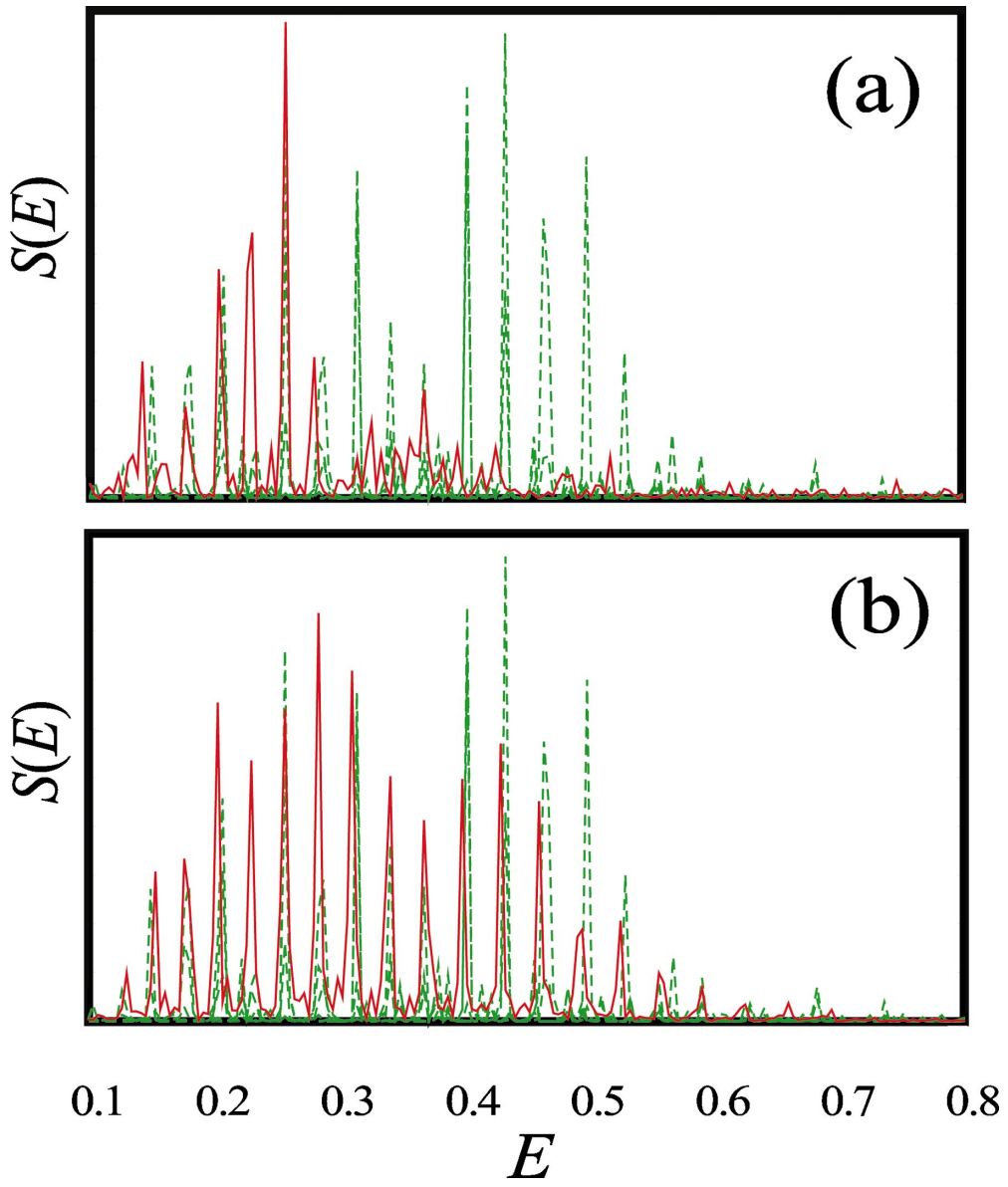

FIG. 4. (Color) (a) Energy spectrum obtained with the normal AFC-II [Eq. (32)] (red and solid line) for the potential $x^2y^2/2 + 0.0025(x^4+y^4)$. Here 500 classical trajectories are picked with an importance sampling technique to mimic the function of Eq. (33) [the energy of the center is 0.505 and $\lambda = 1/(2\hbar)$]. (b) Energy spectrum obtained with the renormalized AFC [Eq. (34)] (red and solid line). The same 500 classical trajectories as above along with their rescaled copies have been used in the energy range from $E = 0.3$ to 1.3 (see text). The green and dotted curves represent quantum spectra (see the text).

random sampling technique to pick trajectories from the one-parameter families of such bound trajectories, since the measure of these families is generally very small in phase space. Under such a situation, it is extremely difficult to realize sufficient constructive and destructive interferences to quantize the vibronic energy levels. It was a great mystery for us why quantum mechanics can describe the bound state of H_2^+ easily under such a very poor classical and quantum correspondence. [The situation becomes more and more tough for electron substituted systems $(p^+p^+\mu^-)$ and $(p^+p^+p^-)$.] The use of the scale invariance may give an answer to this fundamental question. We will report the results of the semiclassical quantization of $(p^+p^+e^-)$ in terms of the renormalized AFC elsewhere [25].

ACKNOWLEDGMENTS

The authors thank K. Hotta for valuable discussions. This work has been supported in part by the Grant-in-Aid for Basic Science (A) and the 21st Century COE Program for Frontiers in Fundamental Chemistry from the Ministry of Education, Culture, Sports, Science and Technology of Japan.

[1] M. C. Gutzwiller, J. Math. Phys. **11**, 1791 (1970); **12**, 343 (1971).
[2] M. C. Gutzwiller, *Chaos in Classical and Quantum Mechanics* (Springer, Berlin, 1990).
[3] P. Gaspard, D. Alonso, and I. Burghardt, Adv. Chem. Phys. **90**, 105 (1995).
[4] A. Inoue-Ushiyama and K. Takatsuka, Phys. Rev. A **60**, 112 (1999).
[5] L. D. Landau and E. M. Lifshitz, *Mechanics* (Addison-Wesley, New York, 1960).
[6] W. H. Miller, J. Chem. Phys. **53**, 3578 (1970).
[7] W. H. Miller, J. Phys. Chem. A **105**, 2942 (2001).
[8] Y. Zhao and W. H. Miller, J. Chem. Phys. **117**, 9605 (2002).
[9] E. J. Heller, J. Chem. Phys. **94**, 2723 (1991).
[10] M. A. Sepúlveda and E. J. Heller, J. Chem. Phys. **101**, 8004 (1994); M. A. Sepúlveda and F. Grossmann, Adv. Chem. Phys. **96**, 191 (1996).
[11] G. Campolieti and P. Brumer, Phys. Rev. A **50**, 997 (1994); D. Provost and P. Brumer, Phys. Rev. Lett. **74**, 250 (1995).
[12] K. G. Kay, J. Chem. Phys. **100**, 4377 (1994); **100**, 4432 (1994).
[13] A. Inoue-Ushiyama and K. Takatsuka, Phys. Rev. E **64**, 056223 (2001).
[14] K. Takatsuka, Phys. Rev. E **64**, 016224 (2001).
[15] K. Hotta and K. Takatsuka, J. Phys. A **36**, 4785 (2003).
[16] H. Goldstein, *Classical Mechanics* (Addison-Wesley, New York, 1980).
[17] K. Takatsuka and A. Inoue, Phys. Rev. Lett. **78**, 1404 (1997); A. Inoue-Ushiyama and K. Takatsuka, Phys. Rev. A **59**, 3256 (1999).
[18] H. Ushiyama, Y. Arasaki, and K. Takatsuka, Chem. Phys. Lett. **346**, 169 (2001).
[19] K. Takatsuka, J. Comput. Phys. **102**, 374 (1992).
[20] R. Loudon, Am. J. Phys. **27**, 649 (1959).
[21] B. Eckhardt, G. Hose, and E. Pollak, Phys. Rev. A **39**, 3776 (1989).
[22] K. G. Kay, J. Chem. Phys. **101**, 2250 (1994).
[23] G. Campolieti and P. Brumer, J. Chem. Phys. **109**, 2999 (1998).
[24] S. Takahashi and K. Takatsuka, Phys. Rev. A **69**, 022110 (2004).
[25] S. Takahashi and K. Takatsuka (unpublished).